JOURNAL OF THE KOREAN ASTRONOMICAL SOCIETY
35: 123 ~ 130, 2002

IRON LINE PROFILES FROM RELATIVISTIC ELLIPTICAL ACCRETION DISKS

HEON-YOUNG CHANG[1] AND CHUL-SUNG CHOI[2]
[1]Korea Institute for Advanced Study, Seoul, Korea 130-012
E-mail: hyc@ns.kias.re.kr
[2]Korea Astronomy Observatory, Taejon, Korea 305-348
E-mail: cschoi@kao.re.kr
(Received Jun. 19, 2002; Accepted Aug. 20, 2002)

ABSTRACT

An elliptical accretion disk may be formed by tidally disrupted debris of a flying-by star in an active galactic nucleus (AGN) or by tidal perturbation due to a companion in a binary black hole system. We investigate the iron Kα line profiles expecting from a geometrically thin, relativistic, elliptical disk in terms of model parameters, and find that a broad and skewed line profile can be reproduced well. Its shape is variable to the model parameters, such as, the emissivity power-law index, the ellipticity of the disk, and the major axis orientation of the elliptical accretion disk. We suggest that our results may be useful to search for such an elliptical disk and consequently the tidal disruption event.

Key words : accretion – line profiles – relativity – X-rays:spectra – black hole physics

I. INTRODUCTION

It is widely believed that the source of the enormous X-ray power of most AGNs and X-ray binaries is gravitational energy released through an accretion disk around a black hole (Lynden-Bell 1969). These X-rays are often thought to be produced by Compton upscattering of optical/UV seed photons in a hot corona above the inner accretion disk (for Comptonization see, e.g., Seon et al. 1994). In this picture, although the coronal heating mechanism is yet to be settled, a substantial amount of the X-rays irradiates the accretion disk and this feedback process results in various observable components in the energy spectra of AGNs, such as broad fluorescent iron lines at 4 - 7 keV, a Compton reflection hump above 10 keV etc. (e.g., Koratkar & Blaes 1999).

Among these spectral features, the iron lines are particularly useful to diagnose properties of an accretion disk and physical states a central black hole. Fabian et al. (1989) showed that the observed broad iron line of Cyg X-1 can be explained reasonably well by the line emission reprocessed in a cool, relativistic, and circular Keplerian accretion disk. The fluorescent iron Kα line at 6.4 keV is intrinsically narrow and its characteristic energy is dependent on the ionization degree of the reprocessing material. A narrow iron line emitted by an accretion disk around a black hole appears to be broadened and skewed due both to the relativistic motion of an accretion disk and to the strong gravity of the black hole. This interpretation has been strengthened by the observation of the very broad, double-peaked and skewed iron Kα line from MCG−6-30-15 (Tanaka et al. 1995).

In a non-relativistic disk, each radius of the disk produces a symmetric double-peaked line profile corresponding to emission from material approaching and receding. On the other hand, near a black hole, where the orbital velocities of the disk are mildly relativistic, special relativistic beaming enhances the blue peak of the each double-peaked line generated at a given radius (Doppler boost). Summing the line emission from all radii of the relativistic disk could give a skewed and highly broadened line profile in principle. Therefore, the line profile we observe is to be affected by several effects such as the geometry of an accretion disk, relativistic Doppler beaming, the relative contribution of transverse Doppler shift (as a general relativistic effect), and gravitational redshifting effects (e.g., Fabian et al. 2000; Pariev et al. 2001). A spinning black hole is sometimes required to fit the observed very broad emission line with a traditional *circular* Keplerian accretion disk.

In addition to this sort of widely-accepted interpretation for the broad and skewed iron line, there are a number of alternatives involving other physical mechanisms: mildly relativistic outflows (Fabian et al. 1995; Lu & Yu 2001), Comptonization (Misra & Kembhavi 1998; Misra & Sutaria 1999; Martocchia et al. 2002), energetic proton spallation (Skibo 1997). In addition to the alternative scenarios which do not involve a Keplerian accretion disk, one can also envisage models of warped or 'blobby' inhomogeneous disks that can produce asymmetric emission-line profiles (Nandra & George 1994; Karas et al. 2000; Hartnoll & Blackman 2001). The inhomogeneities will boost the emissivity of the disk at selected velocities, resulting in asymmetries in the line profile.

One of remarkable recent observational reports on

Corresponding Author: H.-Y. Chang

the iron Kα line is that the line profile of MCG−6-30-15 is subject to change with either the level of the continuum X-ray flux, or time with a timescale down to a few days (Iwasawa et al. 1996). This result may imply that astrophysical conditions of the inner parts of an accretion disk are rapidly changing with time if the line formation region is limited to the inner accretion disk. However, the detailed cause of the temporal or flux-dependent line variation remains yet to be understood, as well as the source of the hard continuum X-rays (Wilms et al. 2001; Fabian et al. 2002).

There are two aspects to tackle the emission line profile variation in the paradigm of the theory reprocessing accretion disk, that is, the continuum source variation itself and the systematic change in the property of the reprocessing accretion disk. Our present study is motivated by these observational facts and concentrates on the second issue. In this paper, we study iron Kα line profiles which are generated by the irradiation to an elliptical, relativistic accretion disk around a Schwarzschild black hole of mass M. Our calculations show that the very broad, double-peaked and skewed line profile is also predictable from an elliptical relativistic accretion disk without a Kerr black hole. This line profile is also variable according to the model parameters.

An elliptical accretion disk may be formed as a result of the capture and disruption of a flying-by star by a supermassive black hole in a host galaxy, and/or tidal perturbation of the companion to the accretion disk around the primary. The mechanism and outcome of tidal disruption events have been studied theoretically and observationally (e.g., Rees 1988; Loeb & Ulmer 1997; Komossa & Bade 1999; Choi et al. 2002; Donley et al. 2002). While about half of the disrupted stellar debris is ejected and escapes from the influence of the supermassive black hole, the rest of the debris falls into the central supermassive black hole and show flare-like events. The infalling material may form an accretion disk in the form of an eccentric disk due to a low angular momentum of the disrupted star, provided that the trajectory of the star is highly eccentric. The supermassive black hole may also be formed as a result of the merger of host galaxies. For conditions of typical cores of giant ellipticals, the two black holes encounter each other and form a bound system in a relatively short time, of order 10^6 years. The tidal effects of the secondary black hole on an accretion disk around the primary to be analogous to the effects of the tidal field of the secondary star in a close binary system.

II. LINE PROFILE OF ELLIPTICAL DISK

We compute the profiles of the emission line from an elliptical Keplerian disk in the weak field approximation following Eracleous et al. (1995). The model and the profile calculations are summarized below.

The Cartesian axes x', y', z' represent the frame of the disk, chosen so that the disk lies in the (x', y')-plane. The observer's frame is indicated by the Cartesian axes x, y, z, with the observer along the positive $z-$axis at $z = +\infty$. The line of sight ($z-$axis) is inclined with respect to the rotation axis of the disk ($z'-$axis) by an angle i. The calculations have been carried out in polar coordinates (r, θ, ϕ), where the primed angles are measured in the frame of the disk as Cartesian coordinates (see Figure 1 of Eracleous et al. 1995). We adopt units in which $G = c = 1$, with G being the gravitational constant and c being the speed of light. We define the dimensionless radial coordinate $\xi \equiv r/r_g$, where $r_g \equiv GM/c^2$ is the gravitational radius.

The total observed line flux from the disk is given by

$$F = \int d\nu \int d\Omega I_\nu, \tag{1}$$

where $\nu, I_\nu, d\Omega$ are the frequency, specific intensity, and solid angle element as measured in the frame of the observer, respectively. By using the invariance of the quantity I_ν/ν^3, the specific intensity can be transformed to the frame of the emitter. The solid angle $d\Omega$ can be conveniently expressed in terms of the impact parameter at infinity, b, as $d\Omega = b\ db\ d\phi/d^2$, where d is the distance to the source. This expression allows one to deal with the difference caused by light bending between the solid angle in the frame of the disk and the solid angle in the frame of the observer. Subsequently the expression for the total line flux becomes

$$F = \frac{1}{d^2} \int d\nu \int b\ db\ d\phi I_{\nu_e} \left(\frac{\nu}{\nu_e}\right)^3, \tag{2}$$

where now ν_e and I_{ν_e} are the frequency and the specific intensity as measured in the frame of the emitter. The line profile itself is described by the function F_X, which is defined by $F = \int F_X dX$, where $1+X = \nu/\nu_0$, and ν_0 is the rest frequency of the line. That is, X is effectively the redshift and F_X is the line flux per unit redshift interval. From equation (2) and the definition of F_X it reads

$$F_X = \frac{\nu_0}{d^2} \int d\nu \int b\ db\ d\phi I_{\nu_e} \left(\frac{\nu}{\nu_e}\right)^3. \tag{3}$$

Though the impact parameter should be given by a numerical integration of the photon geodesic equation, the impact parameter can be expressed in the weak field approximation in terms of ξ, the dimensionless radial coordinate, as

$$\frac{b}{r} \approx (1 - \sin^2 i \cos^2 \phi')^{1/2} \left[1 + \frac{1}{\xi}\left(\frac{1 - \sin i \cos \phi'}{1 + \sin i \cos \phi'}\right)\right], \tag{4}$$

where the term proportional to ξ^{-1} is the first-order correction for light bending. Using equation (4), and expressing $d\phi'$ in terms of ϕ' with the help of

$$\begin{aligned} \sin \phi' &= \sin \theta \sin \phi \\ \cos \theta &= \sin i \cos \phi', \end{aligned} \tag{5}$$

equation (3) becomes

$$F_X = \frac{M^2 \nu_0 \cos i}{d^2} \int\int \xi \, d\xi \, d\phi' I_{\nu_e} D^3 \Psi(\xi, \phi'), \quad (6)$$

where $\Psi(\xi, \phi')$ is given by

$$\Psi(\xi, \phi') = 1 + \frac{1}{\xi}\left(\frac{1 - \sin i \cos \phi'}{1 + \sin i \cos \phi'}\right), \quad (7)$$

and $D \equiv \nu/\nu_e$ is the Doppler factor, which depends on the positions and velocities of the particles in the disk, as well as on the assumed metric. Assuming that the trajectories are known, so that the Doppler factor can be calculated, and that I_{ν_e} is specified, equation (6) gives the profiles of the emergent emission lines. We note that equation (6) involves the local properties of the emitting region in the disk and the local coordinate system, and gives the profiles of the emission lines as seen in the frame of an observer at infinity.

The Doppler factor can be computed by considering the four-velocity of the emitting particles. The four-momentum of a photon originating at radius r is $p^\alpha = h\nu P^\alpha$ where P^α is given by

$$P^\alpha = \left\{\left(1 - \frac{2M}{r}\right)^{-1}, -\left[1 - \left(\frac{b}{r}\right)^2\left(1 - \frac{2M}{r}\right)\right]^{1/2}, -br^2, 0\right\}. \quad (8)$$

The energy of a photon in the rest frame of the emitter is $h\nu_e = p^\alpha u_\alpha = h\nu P^\alpha u_\alpha$, where u_α is the four-velocity of the emitting particle. Hence, from the definition of the Doppler factor it follows that $D \equiv \nu/\nu_e = 1/P^\alpha u_\alpha$. The explicit expression for the Doppler factor was derived by Chen & Halpern (1989) and Chen, Halpern, & Filippenko (1989). We assume that the elliptical disk is made up of elliptical annuli. Each annulus is described by its pericenter distance $\tilde{\xi}$, and its ellipticity e. It is assumed that all annuli share a common major axis, which makes an angle ϕ_0 with the x'-axis. The trajectory of a particle in a given annulus is described by

$$\tilde{\xi}(\phi') = \frac{\tilde{\xi}(1+e)}{1 - e\cos(\phi' - \phi_0)}. \quad (9)$$

The line-emitting part of the disk is bound by inner and outer elliptical annuli of pericenter distances $\tilde{\xi}_1$ and $\tilde{\xi}_2$, respectively. Then, one obtains the following expression for the Doppler factor

$$\frac{1}{D} = \gamma\left\{\left(1 - \frac{2}{\xi}\right)^{-1/2} - \frac{[1 - (b/r)^2(1 - 2/\xi)]^{1/2} e \sin(\phi' - \phi_0)}{\xi^{1/2}(1 - 2/\xi)^{3/2}[1 - e\cos(\phi' - \phi_0)]^{1/2}} + \frac{(b/r)[1 - e\cos(\phi' - \phi_0)]^{1/2} \sin i \sin \phi'}{\xi^{1/2}(1 - 2/\xi)^{1/2}(1 - \sin^2 i \cos^2 \phi')^{1/2}}\right\}, \quad (10)$$

where

$$\gamma = \left\{1 - \frac{e^2 \sin^2(\phi' - \phi_0) + (1 - 2/\xi)[1 - e\cos(\phi' - \phi_0)]^2}{\xi(1 - 2/\xi)^2[1 - e\cos(\phi' - \phi_0)]}\right\}^{-1/2}. \quad (11)$$

We have adopted a prescription for the specific intensity of the line given by

$$I_{\nu_e} = \frac{1}{4\pi} \frac{\epsilon_0 \xi^{-q}}{\sqrt{2\pi}\sigma} \exp\left[-\frac{(\nu_e^2 - \nu_0^2)}{2\sigma^2}\right], \quad (12)$$

where $\epsilon(\xi) = \epsilon_0 \xi^{-q}$ is the line emissivity. In this prescription, the local broadening is represented by a Gaussian profile in the frame of the emitter. The width of the local profile is determined by the broadening parameter σ, which can also be expressed in velocity units via $v_\sigma = c\sigma/\nu_0$. The adopted line emissivity varies with the radial distance from the central object. This is a reasonable parameterization if, for example, the line emission from the disk is driven by illumination from a central extended source of ionizing radiation, in which case one would expect $\epsilon(\xi) \propto \xi^{-3}$. It is, however, necessary to say that the geometry of the inner accretion disk surrounding a black hole is poorly understood and the corresponding line emissivity as a function of radius is unknown yet.

To sum up, the model has seven free parameters, that is, the inner and outer pericenter distances of the elliptical disk (ξ_1, ξ_2), the inclination angle of the disk (i), the assumed emissivity power-law index (q), the broadening parameter (σ), the ellipticity of the disk (e), and the major axis orientation of the elliptical rings (ϕ_0). As noted in the case of circular disks, the profile shapes of the X-ray emission lines are not very sensitive to the broadening parameter, nor the outer pericenter distances. Hence we fix these parameters to presumed values. The ellipticity is also assumed to be constant and uniform throughout the disk in examples shown in this study. However, the latter assumption may have to be relieved as discussed later since circularization and apsidal motion may occur in a different timescale as a function of pericenter distances and the mass of the central object.

III. RESULTS

In order to explore the iron line profiles produced by the elliptical disk and to investigate how they are affected by changes in the model parameters, we have computed a series of model profiles for different combinations of parameters. In Figure 1, we show several examples of line profiles varying with the major axis orientation. All other parameters are fixed : $\xi_1 = 3, \xi_2 = 100, e = 0.5, q = 3.0, i = 32°, \sigma = 800$ km s^{-1}. The disk size is generally of the order of thousand gravitational radii, which is larger than the value we took. We note, however, the results are not very sensitive to

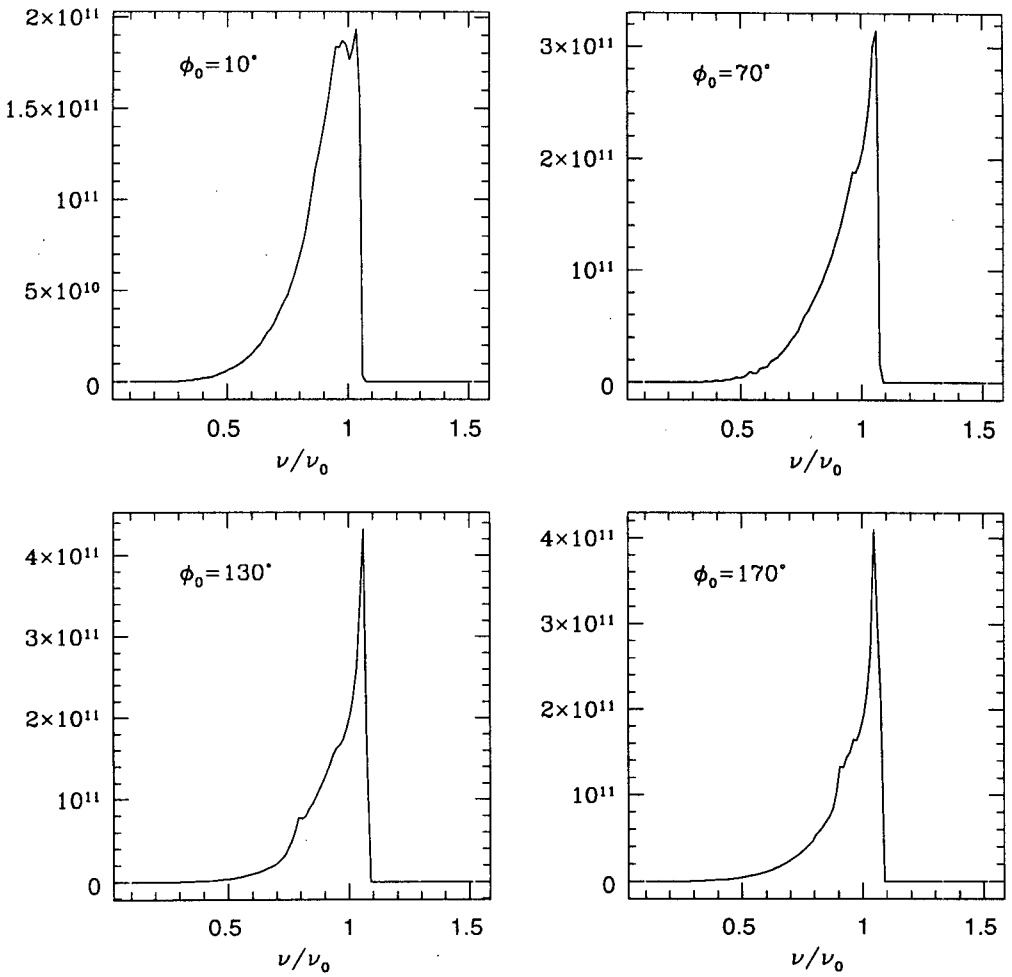

Fig. 1.— Examples Kα line profiles showing the effects of the major axis orientation while other values are fixed. Adopted parameters are as follows: $\xi_1 = 3, \xi_2 = 100, e = 0.5, q = 3.0, i = 32°, \sigma = 800$ km s^{-1}. As the the major axis orientation increases in our coordinate system, the redder peak moves redward and diminishes while the bluer peak relatively unchanges. Note that fluxes are all arbitrarily normalized.

this upper bound. On the other hand, the redward extent of the line is a very sensitive function of the inner radius of the line-emitting annulus. Since the last stable orbit value depends on the angular momentum of the black hole, a suggested ξ_1 value smaller than 3 is often used to support the existence of the rotating black hole. The width, or the redshift extent of the line, however, is also seen to vary with the major axis orientation. Therefore, the observed ξ_1 smaller than 3 may not be a confirmation of the existence of the rotating black hole. We note that the angle changes the energy and the height of the secondary peak more than those of the primary peak.

In Figure 2, we show examples of line profiles showing the effects of various combinations of model parameters for a given major axis orientation. The ellipticity seems to have similar effects as the major axis orientation. As the ellipticity increases the redward peak becomes smaller and moves to the left so that the line width becomes larger. Note that the circular disk corresponds to the case $e = 0$. It should be noted that the position of the blue peak is a more sensitive function of the inclination of the disk with respect to the line of sight, than the red peak as in the case of a circular disk. We find that the effect of q is also not negligible. Since the emissivity power-law index is model-dependent, one may attempt to fit the model profile to the observed data once effects of other model parameters are understood. According to the theoretical studies the different emission mechanisms result in different emissivity power-law index. Therefore, the emissivity power-law index by line profile fitting may help to resolve emission

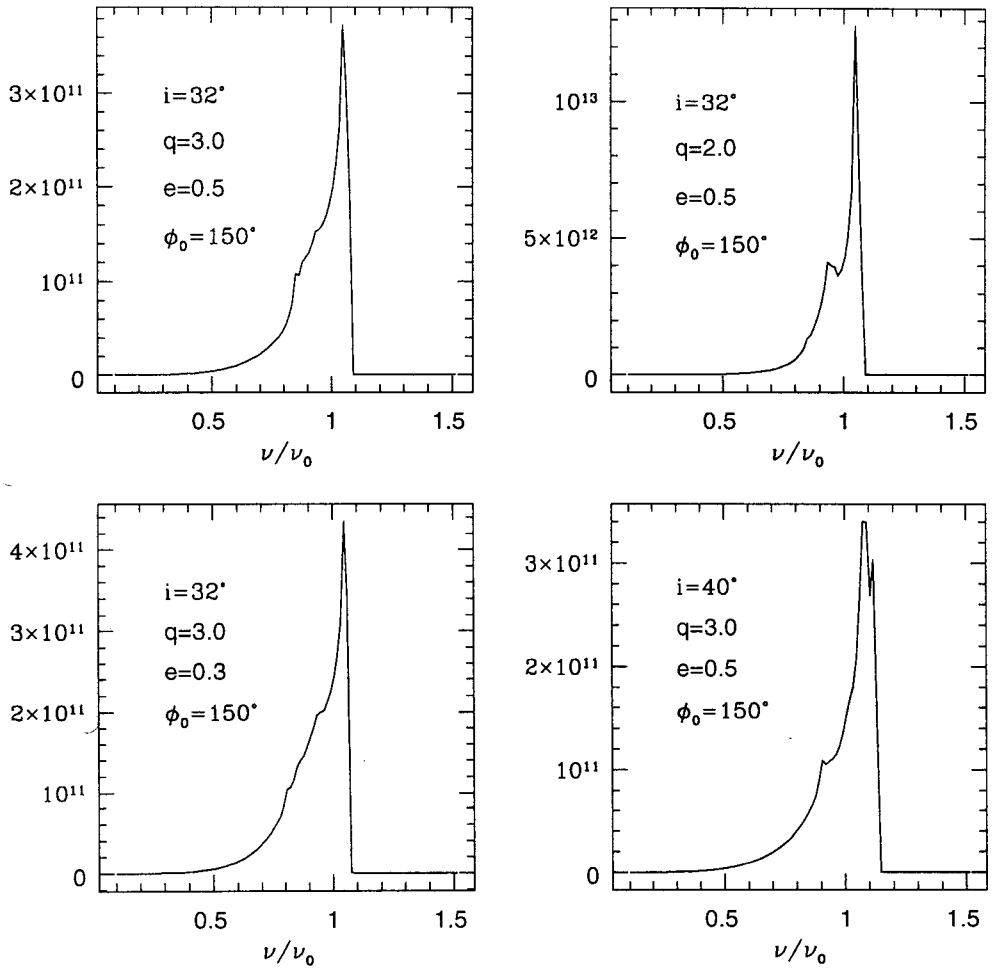

Fig. 2.— Examples Kα line profiles showing the effects of adopted model parameters for a fixed major axis orientation. Adopted parameters are as follows: $\xi_1 = 3, \xi_2 = 100, \sigma = 800$ km s^{-1}, other values are specified in the panels. Note that fluxes are all arbitrarily normalized.

mechanism issues.

The elliptical accretion disk is likely to be subject to the precessing and/or apsidal motions. The timescale is dependent on the mass of the central object and the ellipticity. The precession period due to a Schwarzschild black hole is given by $P_{\rm GR} \sim 10 M_6 \tilde{\xi}_3^{5/2}$ years (Weinberg 1972), where M_6 is the mass in units of $10^6 M_\odot$, $\tilde{\xi}_3$ is $\tilde{\xi}/10^3$. On the other hand, the precession period due to the tidal effect of the secondary in a binary black hole is given by $P_{\rm Bin} \sim 5000(q_4^3/(1+q_4))a_{17}^{3/2} M_6^{-1/2}$ years, where q_4 is the mass ratio in units of 4, a is the semimajor axis in units of 10^{17} cm (Eracleous et al. 1995). For a close binary system case, the observational duration can be comparable with or even longer than the period of the apsidal motion. In this case, the observed line profile should be an average of line profiles over the period of the apsidal motion. In Figure 3, we show the averaged line profiles over the apsidal motion are shown. General features are more or less similar to those shown in Figure 2. As mentioned in the last section circularization may take place in different timescales for different elliptical annuli so that the assumption on the common ellipticity and major axis orientation may break down in this case where the period of the apsidal motion is short.

IV. SUMMARY AND DISCUSSION

An elliptical disk can be formed either resulting from the tidal disruption of a star by the central supermassive black hole or due to tidal perturbation of the secondary companion black hole on the disk. If any of the observed double-peaked emission lines do indeed arise

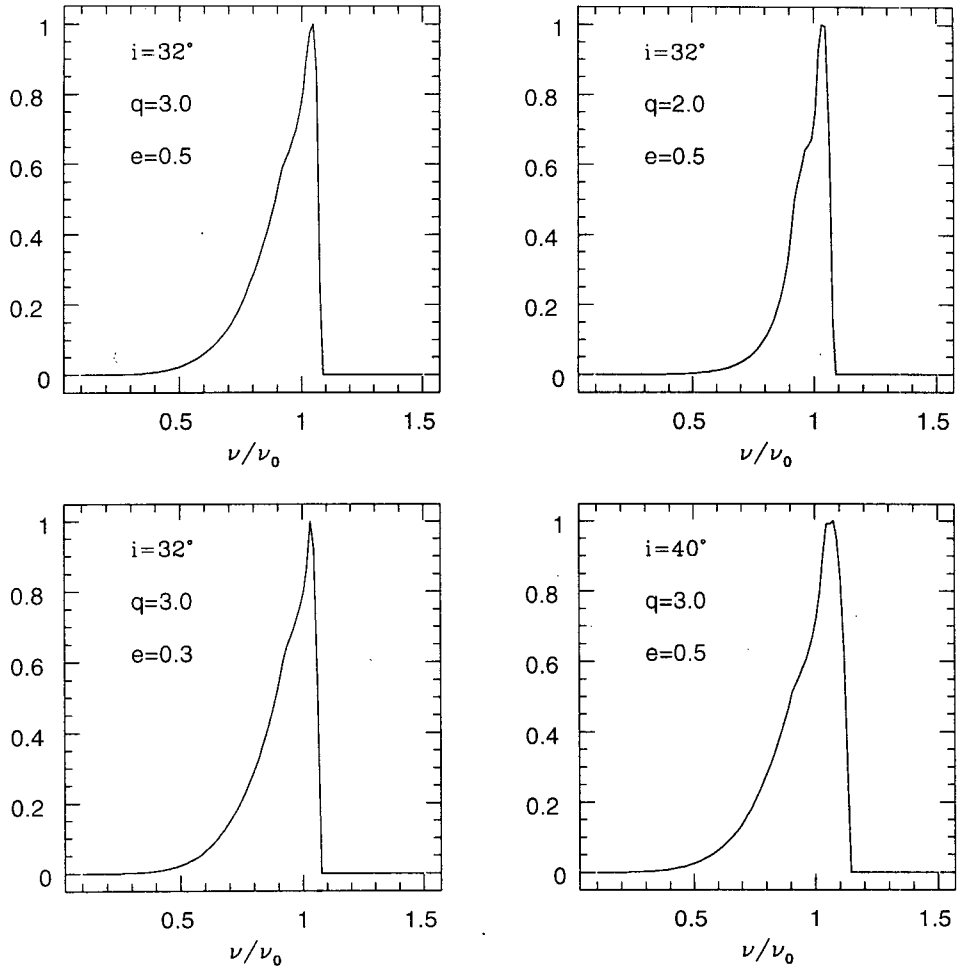

Fig. 3.— Averaged Kα line profiles over the complete apsidal motions, assuming observational duration is longer than the apsidal period. Adopted parameters are as follows: $\xi_1 = 3, \xi_2 = 100, \sigma = 800$ km s^{-1}, other values are specified in the panels. Note that fluxes are all arbitrarily normalized.

in an elliptical disk, their profiles are likely to vary due to apsidal motions of the disk. We present a calculation of the profiles of emission lines originating in a relativistic, elliptical disk, and show examples of the resulting model profiles. We demonstrate that such a disk can reproduce a very broad, skewed line profile reasonably well without a rotating black hole in the center of the disk and that the shape of the line depends on a combination of model parameters. Particularly, the major axis orientation seems to play a role of the innermost stable orbit. Therefore, the redward extent of the line cannot be a conclusive evidence for the existence of the spinning black hole and the variability in the line profile can be explained with an apsidal motion of the elliptical disk.

We, however, should also mention a few shortcomings. Firstly, the particle trajectories in the inner parts of the disk can become circular fast, due both to the apsidal motion and to the differential precession of the orbits very close to the black hole. The circularization timescale of the disk due to relativistic differential precession is given by $\tau_{\rm circ} \sim 2 \times 10^2 M_6 T_5^{-1/2}(1+e)\tilde{\xi}_2^2$ years, where T_5 is the local temperature in units of 10^5 K, $\tilde{\xi}_3$ is $\tilde{\xi}/10^3$ (Eracleous et al. 1995). Therefore, results of the calculation above can only be applicable to a system either where a companion permanently, or longer than the life time of the disk, the accretion disk system, or (closely) immediately after when the accretion disk forms, such as tidal disruption events. Secondly, it should include a numerical integration of the photon geodesic equation in a Schwarzschild metric which is relevant for photon impact parameters $\leq 10 r_s$, where most of X-rays originate. The light bending ap-

proximation, which we adopted in this study, is ≥ 10 percent inaccurate within this region (see Fabian et al. 1995). Thirdly, other forms of accretion disk involving geometrically and/or physically different properties should be also considered to study line variability for completeness (e.g., Park 2001; Chang 2001).

The elliptical disk model may not be applicable to explain the line profile variation of most AGNs in reality, because of the rapid circularization of the disk. However, our result instead may be useful to search for some exotic events of AGNs, e.g., the tidal disruption event. It has long been suggested that flare or outburst could be induced by the tidal disruption event of a star by a supermassive black hole resides in the center of an AGN (Rees 1988). Several researchers have also argued that unusual outbursts and/or intermittent flares observed in some of long-term X-ray light curves of AGNs could be interpreted as the result of the tidal disruption event, where the luminosity increases from a factor of a few to 3 orders of magnitude during the flares or outbursts and they last for a few years (e.g., Komossa & Bade 1999; Komossa & Greiner 1999; Choi et al. 2001, 2002; Donley et al. 2002). However, with these observational results alone, it is still difficult to confirm that the tidal disruption event is responsible for the observed phenomena, because of lack of spectral information for the event. We here suggest that if information on the emission lines is available, it could be firm evidence of the existence of such an elliptical system and consequently the tidal disruption event. In principle this is possible if we monitor the iron line-profile evolution periodically after detecting an X-ray outburst. Of course, an instrument having a sufficient energy resolution and sensitivity should be given for this observation. We expect that the iron line could be broader because of a transient elliptical disk formed due to debris of stellar objects and could also be varying systematically due to its apsidal motion though its timescale is uncertain. To make a comparison between calculation and observation of the iron line in details, more complex and realistic disk geometry should also be considered in the profile calculations as mentioned in § II. This is beyond the scope of the present study.

ACKNOWLEDGEMENTS

We thank the referees for useful comments which improve our original manuscript. HYC thanks Hee-Won Lee for discussions on the line formation of symbiotic stars, by which calculations of the line profile due to an accretion disk were stimulated.

REFERENCES

Chang, H. -Y. 2001, Can a wind model mimic a convection-dominated accretion flow model?, JASS, 18, 1

Chen, K., & Halpern, J. P. 1989, Structure of line-emitting accretion disks in active galactic nuclei - ARP 102B, ApJ, 344, 115

Chen, K., Halpern, J. P., & Filippenko, A. V. 1989, Kinematic evidence for a relativistic Keplerian disk - ARP 102B, ApJ, 339, 742

Choi, C. -S., Dotani, T., Yi, I., Fletcher, A., & Kim, C. 2001, X-ray archival data analysis of time variabilities in seyfert galaxy MCG−2-58-22, JKAS, 34, 129

Choi, C. -S., Dotani, T., Chang, H. -Y., & Yi, I. 2002, Long-term X-ray variabilities of the seyfert galaxy MCG−2-58-22: secular flux decrease and flares, JKAS, 35, 1

Donley, J. L., Brandt, W. N., Eracleous, M., & Boller, T. 2002, Large-amplitude X-ray outbursts from galactic nuclei: a systematic survey using ROSAT archival data, astro-ph/0206291

Eracleous, M., Livio, M., Halpern, Jules P., & Storchi-Bergmann, T. 1995, Elliptical accretion disks in active galactic nuclei, ApJ, 438, 610

Fabian, A. C., Iwasawa, K., Reynolds, C. S., & Young, A. J. 2000, Broad iron lines in active galactic nuclei, PASP, 112, 1145

Fabian, A. C., Nandra, K., Reynolds, C. S., Brandt, W. N., Otani, C., Tanaka, Y., Inoue, H., & Iwasawa, K. 1995, On broad iron Kalpha lines in Seyfert 1 galaxies, MNRAS, 277, L11

Fabian, A. C., Rees, M. J., Stella, L., & White, N. E. 1989, X-ray fluorescence from the inner disc in Cygnus X-1, MNRAS, 238, 729

Fabian, A. C., Vaughan, S., Nandra, K., Iwasawa, K., Ballantyne, D. R., Lee, J. C., De Rosa, A., Turner, A., & Young, A. J. 2002, A long hard look at MCG−6-30-15 with XMM-Newton, astro-ph/0206095

Hartnoll, S. A., & Blackman, E. G. 2001, Reprocessed emission line profiles from dense clouds in geometrically thick accretion engines, MNRAS, 324, 257

Iwasawa, K., Fabian, A. C., Reynolds, C. S., Nandra, K., Otani, C., Inoue, H., Hayashida, K., Brandt, W. N., Dotani, T., Kunieda, H., Matsuoka, M., & Tanaka, Y. 1996, The variable iron K emission line in MCG−6-30-15, MNRAS, 282, 1038.

Karas, V., Czerny, B., Abrassart, A., & Abramowicz, M. A. 2000, A cloud model of active galactic nuclei: the iron Kα line diagnostics, MNRAS, 318, 547

Komossa, S., & Bade, N. 1999, The Giant X-ray outburst in NGC 5905 and IC 3599, A&A, 343, 775

Komossa, S., & Greiner, J. 1999, Discovery of a giant and luminous X-ray outburst from the optically inactive galaxy pair RXJ1242.6-1119, A&A, 349, L45

Koratkar, A., & Blaes, O. 1999, The ultraviolet and optical continuum emission in active galactic nuclei: the status of accretion disks, PASP, 111, 1

Loeb, A., & Ulmer, A. 1997, Optical appearance of the debris of a star disrupted by a massive black hole, ApJ, 489, 573

Lu, Y., & Yu, Q. 2001, The effects of relativistic bulk motion of X-ray flares in the corona on the iron Kα line in Seyfert 1 galaxies, ApJ, 561, 660

Lynden-Bell, D. 1969, Galactic nuclei as collapsed old quasars, Nature, 223, 690

Martocchia, A., Matt, G., Karas, V., Belloni, T., & Feroci, M. 2002, Evidence for a relativistic iron line in GRS 1915+105, A&A, 387, 215

Misra, R., & Kembhavi, A. K. 1998, Broadening of the iron emission line in MCG−6-30-15 by comptonization, ApJ, 499, 205

Misra, R., & Sutaria, F. K. 1999, Comparisons of various model fits to the iron line profile in MCG−6-30-15, ApJ, 517, 661

Nandra, K., & George, I. M. 1994, Constraining the complexities in Seyfert X-ray spectra - an analysis of simultaneous observations with GINGA and ROSAT, MNRAS, 267, 193

Pariev, N. I., Bormley, B. C., & Miller, W. A. 2001, Estimation of relativistic accretion disk parameters from iron line emission, ApJ, 547, 649

Park, M. -G. 2001, Relativistic radiation hydrodynamics of spherical accretion, JKAS, 34, 309

Rees, M. 1988, Tidal disruption of stars by black holes of 10 to the 6th-10 to the 8th solar masses in nearby galaxies, Nature, 333, 523

Seon, K. -I., Choi, C. -S., Nam, U. -W., & Min, K. -W., 1994, Monte Carlo simulation of comptonization in a spherical shell geometry, JKAS, 27, 45

Skibo, J. G. 1997, Spallation of iron in black hole accretion flows, ApJ, 478, 522

Tanaka, Y., Nandra, K., Fabian, A. C., Inoue, H., Otani, C., Dotani, T., Hayashida, K., Iwasawa, K., Kii, T., Kunieda, H., Makino, F., & Matsuoka, M. 1995, Gravitationally redshifted emission implying an accretion disk and massive black-hole in the active galaxy MCG−6-30-15, Nature, 375, 659

Weinberg, S. 1972, Gravitation and Cosmology (New York : Wiley), p197

Wilms, J., Reynolds, C. S., Begelman, M. C., Reeves, J., Molendi, S., Stuabert, R., & Kendziorra, E. 2001, XMM-EPIC observation of MCG−6-30-15: direct evidence for the extraction of energy from a spinning black hole?, MNRAS, 328, L27